

Proceedings of the

Advanced Architectures in Photonics

September 21–24, 2014

Prague, Czech Republic

Volume 1

Editors

Jiri Orava

University of Cambridge
Department of Materials Science and Metallurgy
27 Charles Babbage Road
CB3 0FS Cambridge
United Kingdom

Tohoku University
WPI-Advanced Institute for Materials Research
(WPI-AIMR)
2-1-1 Katahira, Aoba-ku
980-8577 Sendai
Japan

Tomas Kohoutek

Involved Ltd.
Siroka 1
537 01 Chrudim
Czech Republic

Proceeding of the Advanced Architectures in Photonics
<http://aap-conference.com/aap-proceedings>

ISSN: 2336-6036
September 2014

Published by **Involved Ltd.**
Address: Siroka 1, 53701, Chrudim, Czech Republic
Email: info@involved.cz, Tel. +420 732 974 096



This work is licensed under a
[Creative Commons Attribution
3.0 Unported License](https://creativecommons.org/licenses/by/3.0/).

CONTENTS

[Preface](#)

T. Wagner (Chairman)	i
----------------------------	---

FULL PAPERS

[Innovative nanoimprint lithography](#)

S. Matsui, H. Hiroshima, Y. Hirai and M. Nakagawa	1
---	---

[Nanofabrication by imprint lithography and its application to photonic devices](#)

Y. Sugimoto, B. Choi, M. Iwanaga, N. Ikeda, H. T. Miyazaki and K. Sakoda	5
--	---

[Soft-mould imprinting of chalcogenide glasses](#)

T. Kohoutek, J. Orava and H. Fudouzi	9
--	---

[Electric nanoimprint to oxide glass containing alkali metal ions](#)

T. Misawa, N. Ikutame, H. Kaiju and J. Nishii	11
---	----

[Producing coloured materials with amorphous arrays of black and white colloidal particles](#)

Y. Takeoka, S. Yoshioka, A. Takano, S. Arai, N. Khanin, H. Nishihara, M. Teshima, Y. Ohtsuka and T. Seki	13
--	----

[Stimuli-responsive colloidal crystal films](#)

C. G. Schafer, S. Heidt, D. Scheid and M. Gallei	15
--	----

[Opal photonic crystal films as smart materials for sensing applications](#)

H. Fudouzi and T. Sawada	19
--------------------------------	----

[Introduction of new laboratory device 4SPIN® for nanotechnologies](#)

M. Pokorny, J. Rebíček, J. Klémes and V. Velebný	20
--	----

[Controlling the morphology of ZnO nanostructures grown by Au-catalyzed chemical vapor deposition and chemical bath deposition methods](#)

K. Govatsi and S. N. Yannopoulos	22
--	----

[Visible photon up-conversion in glassy \$\(\text{Ge}_{25}\text{Ga}_{5}\text{Sb}_{5}\text{S}_{65}\)_{100-x}\text{Er}_x\$ chalcogenides](#)

L. Strizik, J. Zhang, T. Wagner, J. Oswald, C. Liu and J. Heo	27
---	----

POSTERS presented at AAP 2014

[Solution processing of As-S chalcogenide glasses](#)

T. Kohoutek	31
-------------------	----

[Ga-Ge-Sb-S:Er³⁺ amorphous chalcogenides: Photoluminescence and photon up-conversion](#)

L. Strizik, J. Oswald, T. Wagner, J. Zhang, B. M. Walsh and J. Heo	32
--	----

[Multi-wavelength and multi-intensity illumination of the GeSbS virgin film](#)

P. Knotek, M. Kincl and L. Tichý	33
--	----

[Towards functional advanced materials based using filling or ordered anodic oxides supports and templates](#)

J. M. Macak, T. Kohoutek, J. Kolar and T. Wagner	34
--	----

[Introduction of new laboratory device 4SPIN® for nanotechnologies](#)

M. Pokorny, J. Rebíček, J. Klémes and V. Velebný	35
--	----

[Profile and material characterization of sine-like surface relief Ni gratings by spectroscopic ellipsometry](#)

J. Mistrik, R. Antos, M. Karlovec, K. Palka, Mir. Vlcek and Mil. Vlcek	36
--	----

[Preparation of sparse periodic plasmonic arrays by multiple-beam interference lithography](#)

M. Vala and J. Homola	37
-----------------------------	----

[High-performance biosensing on random arrays of gold nanoparticles](#)

B. Spackova, H. Sipova, N. S. Lynn, P. Lebruskova, M. Vala, J. Slaby and J. Homola	38
--	----

Visible photon up-conversion in glassy $(\text{Ge}_{25}\text{Ga}_5\text{Sb}_5\text{S}_{65})_{100-x}\text{Er}_x$ chalcogenides

L. Strizik,^{1,*} J. Zhang,² T. Wagner,¹ J. Hrabovsky,¹ J. Oswald,³ C. Liu⁴ and J. Heo²

¹ Department of General and Inorganic Chemistry, Faculty of Chemical Technology, University of Pardubice, Studentska 573, 53210 Pardubice, Czech Republic

² Division of Advanced Nuclear Engineering, Center for Information Materials, Department of Materials Science and Engineering, Pohang University of Science and Technology (POSTECH), San 31, Hyoja-dong, Pohang, Gyeongbuk 790-784, Republic of Korea

³ Institute of Physics of the ASCR, v.v.i., Cukrovarnicka 10, 16200 Prague, Czech Republic

⁴ State Key Laboratory of Silicate Materials for Architectures, Wuhan University of Technology, 122 Luoshi Road, Hongshan, Wuhan, Hubei 430070, PR China

*Electronic mail: lukas.strizik@centrum.cz

We present a brief study on green and red photon up-conversion emission in $(\text{Ge}_{25}\text{Ga}_5\text{Sb}_5\text{S}_{65})_{100-x}\text{Er}_x$ amorphous chalcogenides ($x = 0.2$ and 0.5 at.%) originating from $^2\text{H}_{11/2} \rightarrow ^4\text{I}_{15/2}$ ($\lambda \approx 530$ nm), $^4\text{S}_{3/2} \rightarrow ^4\text{I}_{15/2}$ ($\lambda \approx 550$ nm) and $^4\text{F}_{9/2} \rightarrow ^4\text{I}_{15/2}$ ($\lambda \approx 660$ nm) electronic transitions within Er^{3+} ions under 802 nm laser pumping. The dependence of photon up-conversion emission on the Er^{3+} ions concentration as well as on the pumping power density is shown and discussed.

Amorphous chalcogenides doped with lanthanide Ln^{3+} ions are attractive materials in wide range of applications, such as up-converters [1, 2], lasers [3, 4], displays [5], light amplifiers [6], sensors and detectors [7, 8], waveguides [9] and optical fibers [10]. The advantages of amorphous chalcogenides as a host matrix are low phonon energy suppressing non-radiative recombination processes, high refractive index promoting radiative electronic transitions, wide transparency window ranging from visible to mid-infrared spectral region and chalcogenides are relatively easy make either in a bulk or thin-film form [11–16].

The frequently studied and promising matrices for hosting Ln^{3+} ions are sulfide glasses such as Ga-Ge-S [1, 17], Ga-La-S [2], Ga-Ge-La-S [18, 19], and recently we also reported Ga-Ge-Sb-S [20]. In all of these intense photon up-conversion from visible spectral region has been achieved. It has been shown that addition of antimony into Ge-Ga-S glass results into excellent resistance to moisture [21, 22], additionally the Sb improves thermal stability [20, 21] and Sb-doped glasses show higher glass-forming ability [20, 21]. In all cases the presence of Ga(III) atoms enhance solubility of Ln^{3+} ions [23, 24].

Usually, the photon up-conversion emission in Er^{3+} -doped glassy sulfides originates from wavelength of $\lambda \sim 500$ nm because of the host matrix fundamental absorption edge at around 500 nm [13, 14] and/or narrowing of Er^{3+} : $^2\text{H}_{9/2}$, $^4\text{F}_{7/2}$, $^2\text{H}_{11/2}$ and $^4\text{S}_{3/2}$ energy levels leading to high probability of multiphonon relaxation [19]. Therefore, the blue photon up-conversion emissions in Er^{3+} -doped chalcogenides originating from Er^{3+} : $^2\text{H}_{9/2} \rightarrow ^4\text{I}_{15/2}$ ($\lambda \approx 410$ nm) transitions has not been observed [19].

In present work, we demonstrate the effect of Er^{3+} concentration and laser pumping power on photon up-conversion emission in visible spectral region.

Absorption spectra of studied samples are shown in the Fig. 1. There is possible to observe intra-4f electronic transitions of Er^{3+} ions from $^4\text{I}_{15/2}$ energy level to higher energy states. The Er^{3+} : $^4\text{I}_{15/2} \rightarrow ^2\text{H}_{11/2}$ (530 nm) and Er^{3+} : $^4\text{I}_{15/2} \rightarrow ^4\text{S}_{3/2}$ (550 nm) electronic transitions are close to absorption edge of studied samples. It should be mentioned that the thickness of both samples is same and thus, it is possible to observe a slight red shift of absorption edge with increase of Er^{3+} ions concentration.

Up-conversion emission spectra of $(\text{Ge}_{25}\text{Ga}_5\text{Sb}_5\text{S}_{65})_{100-x}\text{Er}_x$, where $x = 0.2$ and 0.5 at% Er^{3+} excited by 802 nm cw Ti:sapphire laser in dependence of pumping power are shown in the Fig. 2. Both spectra in the Fig. 2 show up-conversion emission bands originating from Er^{3+} : $^2\text{H}_{11/2} \rightarrow ^4\text{I}_{15/2}$ (≈ 530 nm), Er^{3+} : $^4\text{S}_{3/2} \rightarrow ^4\text{I}_{15/2}$ (≈ 550 nm) and Er^{3+} : $^4\text{F}_{9/2} \rightarrow ^4\text{I}_{15/2}$ (≈ 660 nm) intra-4f electronic transitions. It can be observed that the up-conversion emission intensity increases with increase of the pumping power. However, this is not true in the case of Er^{3+} : $^4\text{S}_{3/2} \rightarrow ^4\text{I}_{15/2}$ (≈ 550 nm) electronic emission transitions in a sample with $x = 0.2$ at% Er^{3+} ions where it is possible to observe decrease of the emission intensity with increase of the pumping power from 300 mW.

Green ($\approx 530, 550$ nm) up-conversion emission intensity in $(\text{Ge}_{25}\text{Ga}_5\text{Sb}_5\text{S}_{65})_{99.8}\text{Er}_{0.2}$ sample is comparable with red up-conversion emission intensity (≈ 660 nm) as is shown in Fig. 2. However, in the $(\text{Ge}_{25}\text{Ga}_5\text{Sb}_5\text{S}_{65})_{99.5}\text{Er}_{0.5}$ sample, red up-conversion emission intensity dominates over green up-conversion emission at higher pumping

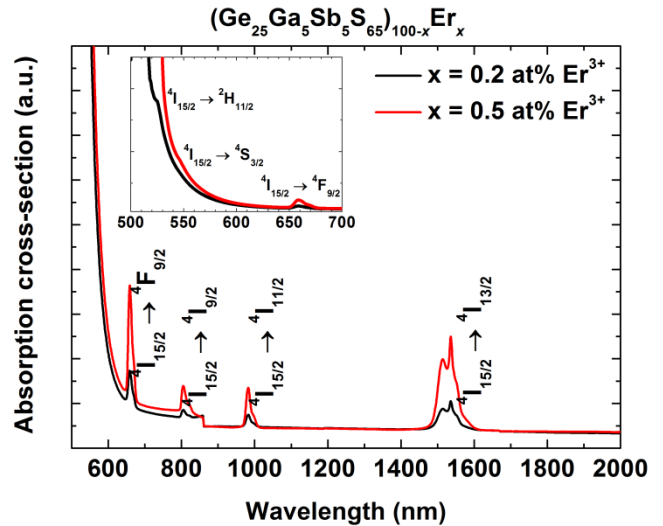


Figure 1. Absorption cross-section of $(\text{Ge}_{25}\text{Ga}_5\text{Sb}_5\text{S}_{65})_{100-x}\text{Er}_x$ amorphous chalcogenides, where $x = 0.2$ and 0.5 at%. The feature close to 850 nm is an instrument error.

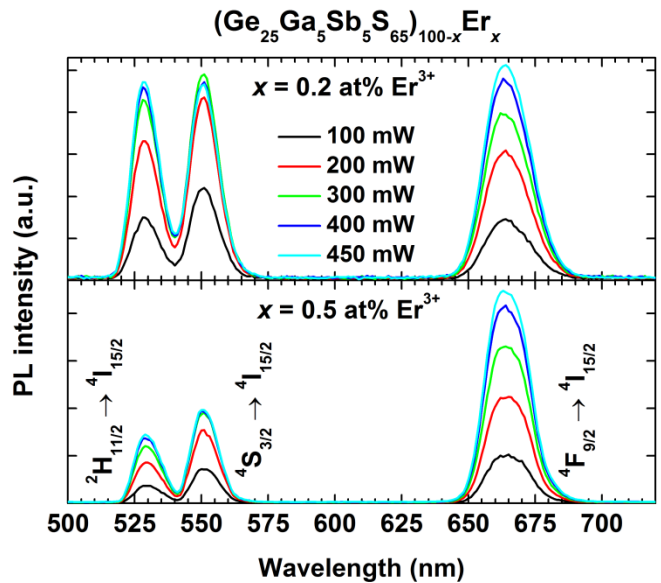


Figure 2. Green and red photon up-conversion emission spectra of $(\text{Ge}_{25}\text{Ga}_5\text{Sb}_5\text{S}_{65})_{100-x}\text{Er}_x$ amorphous chalcogenides under 802 nm Ti:sapphire laser pumping at various pumping powers.

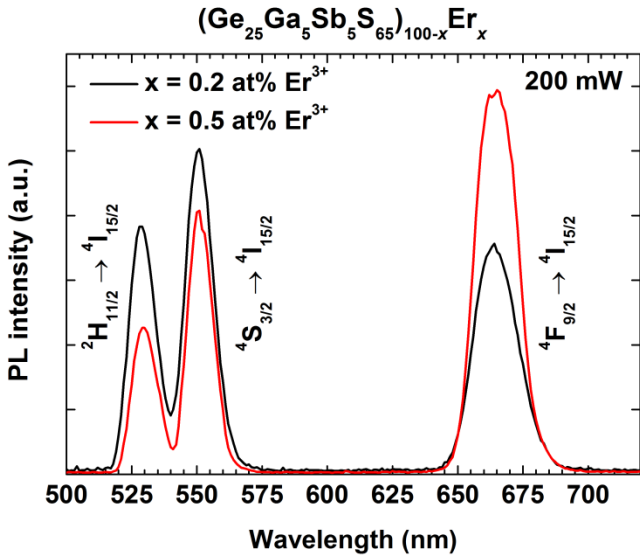


Figure 3. Green and red photon up-conversion emission spectra of $(\text{Ge}_{25}\text{Ga}_5\text{Sb}_5\text{S}_{65})_{100-x}\text{Er}_x$ amorphous chalcogenides under 802 nm Ti:sapphire laser pumping at a pumping power of 200 mW. Spectra are normalized per unity area.

powers. This statement is supported with the up-conversion emission spectra at the pumping power of 200 mW showed in Fig. 3, these spectra are normalized per unit area. Fig. 3 demonstrates higher green and lower red up-conversion emission intensities of the sample doped with 0.2 at% Er^{3+} ions in comparison with the sample doped with 0.5 at% Er^{3+} ions. This behavior can be assigned to changes in Er^{3+} inter-ionic distances with increase of Er^{3+} concentration [15]. At higher concentration of Er^{3+} ions the energy transfer processes can play a significant role in up-conversion emission [25].

Log-log plot of dependence of up-conversion emission intensity I versus pumping power density P can clarify the present up-conversion mechanism because these quantities are related each to other as $I \propto P^n$, where n is number of photons acting in up-conversion process [26]. Mentioned dependencies for green Er^{3+} : ${}^2\text{H}_{11/2}$, ${}^4\text{S}_{3/2} \rightarrow {}^4\text{I}_{15/2}$ ($\lambda = 510\text{--}580$ nm) and red Er^{3+} : ${}^4\text{F}_{9/2} \rightarrow {}^4\text{I}_{15/2}$ ($\lambda = 640\text{--}700$ nm) photon up-conversion emissions of $(\text{Ge}_{25}\text{Ga}_5\text{Sb}_5\text{S}_{65})_{100-x}\text{Er}_x$ samples at pumping wavelength of 802 nm are presented in the Fig. 4. The number of photons n involved in up-conversion process can be derived from the slope of linear fit to appropriate data points [26]. The slopes between 100 and 200 mW are approximately $n \approx 1$ which does not correspond to a theoretical prediction of $n \approx 2$. Higher pumping powers than 200 mW lead to reduction of n in green photon up-conversion emission from $n \approx 1.0\text{--}1.1$ to $n \approx 0.3\text{--}0.5$ and also for a red photon up-conversion emission of the sample doped with 0.2 at% Er^{3+} ions from $n \approx 1.1$ to $n \approx 0.6$.

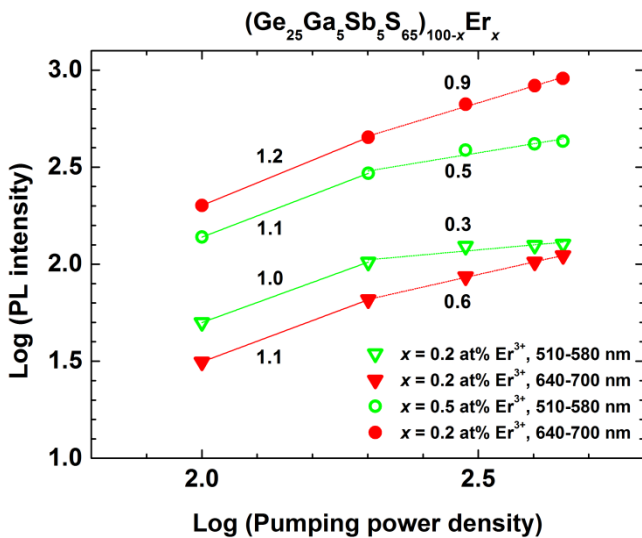


Figure 4. Log-log plot of the green ($\lambda \approx 510\text{--}580$ nm) and red ($\lambda \approx 640\text{--}700$ nm) photon up-conversion emission intensity as a function of the 802 nm laser pumping power and Er^{3+} concentration in $(\text{Ge}_{25}\text{Ga}_5\text{Sb}_5\text{S}_{65})_{100-x}\text{Er}_x$ amorphous chalcogenides.

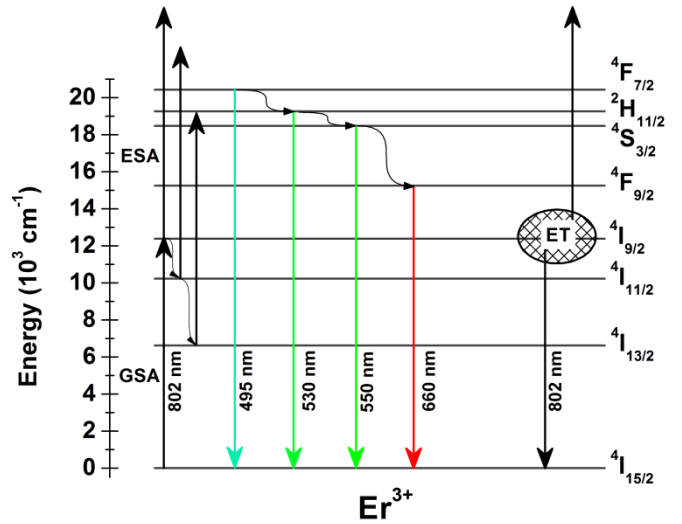


Figure 5. Er^{3+} energy level diagram with highlighted possible excitation transition routes (black straight arrows) in $(\text{Ge}_{25}\text{Ga}_5\text{Sb}_5\text{S}_{65})_{100-x}\text{Er}_x$ at pumping wavelength of 808 nm, possible routes of multiphonon relaxation processes (black curved arrows) and up-conversion emission transitions (colored arrows). GSA denotes Ground State Absorption mechanism, ESA denotes Excited State Absorption mechanism and ETU denotes possible Energy Transfer route.

We assume that in photon up-conversion mechanism there is present two-photon absorption process in the meaning of ${}^4\text{I}_{15/2} \rightarrow {}^4\text{I}_{9/2} \rightarrow {}^2\text{H}_{11/2}({}^4\text{F}_{7/2})$ when the multiphonon relaxation is neglected. However, this phenomenon will play an important role in the population of ${}^2\text{H}_{11/2}$, ${}^4\text{S}_{3/2}$ and ${}^4\text{F}_{9/2}$ energy levels at pumping wavelength of 802 nm as it is depicted using an energy level diagram shown in Fig. 5. Thus, the proposed multiphonon route is $({}^4\text{F}_{7/2}) \rightarrow {}^2\text{H}_{11/2} \rightarrow {}^4\text{S}_{3/2} \rightarrow {}^4\text{F}_{9/2}$. It should be mentioned that energies of ${}^2\text{H}_{11/2}$, ${}^4\text{F}_{7/2}$ levels lie close to the optical band gap energy of the host matrix and thus, the reabsorption processes can also affect the photon up-conversion emission. The absence of one photon in experimentally observed data, Fig. 4, may correspond to photon up-conversion process driven by the intermediate level branching kinetics as was demonstrated for $\text{Cs}_3\text{Lu}_2\text{Cl}_9:\text{Er}^{3+}$ in [25–27] when the GSA/ETU (Ground State Absorption/Energy Transfer Up-conversion) mechanism is present [25]. Then, at high-power excitation, the GSA/ETU intensity exhibits a non-quadratic behavior in double logarithmic dependence on the pumping power [25]. The saturation effect is not excluded as well as the presence of GSA/ESA (Ground State Absorption/Excited State Absorption) mechanism [25, 28]. The non-linear shape of double logarithmic dependence, Fig. 3, may also be related to the beam shape of excitation laser which is Gaussian and thus can lead to a non-uniform distribution of the pump power over the sample volume [26]. For detail understanding of these phenomena, the rate equations

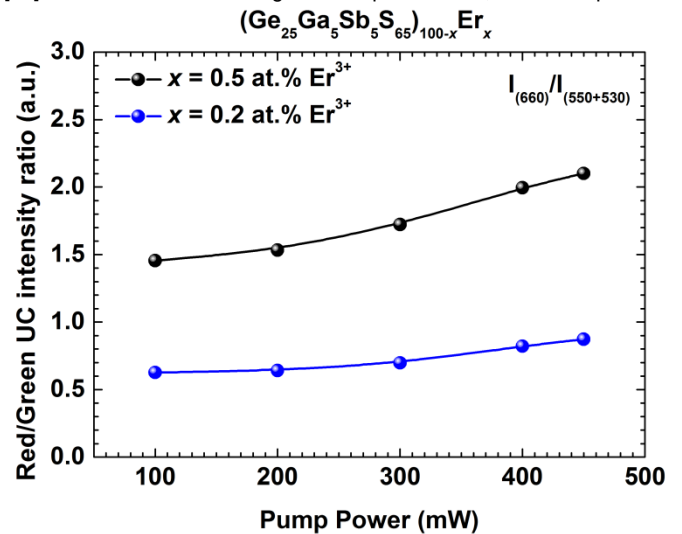


Figure 6. Integrated red-to-green up-conversion emission bands ratio as a function of the 802 nm laser pumping power and Er^{3+} ions concentrations in $(\text{Ge}_{25}\text{Ga}_5\text{Sb}_5\text{S}_{65})_{100-x}\text{Er}_x$ amorphous chalcogenides.

in combination with kinetic measurement of up-conversion emission as well as measurement at lower pumping powers may lead to a solution of studied problematic [25].

Fig. 6 represents the emission intensity ratios of red-to-green photon up-conversion emission bands area in dependence of the pumping power density. There is clear tendency in increase of red photon up-conversion intensity with increase of pumping power and with increase of Er^{3+} ions concentration. The concentration dependent behavior was interpreted e.g. in [29] as a consequence of thermal effect during the exposure of the beam with the laser beam at high powers.

Stokes emission spectra of the $(\text{Ge}_{25}\text{Ga}_5\text{Sb}_5\text{S}_{65})_{100-x}\text{Er}_x$ samples, where $x = 0.2$ and 0.5 at% Er^{3+} , are shown in Fig. 7. There is possible to observe Er^{3+} : $^4\text{I}_{11/2} \rightarrow ^4\text{I}_{15/2}$ (990 nm), Er^{3+} : $^4\text{I}_{13/2} \rightarrow ^4\text{I}_{15/2}$ (1.5 μm) and Er^{3+} : $^4\text{I}_{9/2} \rightarrow ^4\text{I}_{13/2}$ (1.7 μm) electronic emission transitions under 802 nm laser pumping.

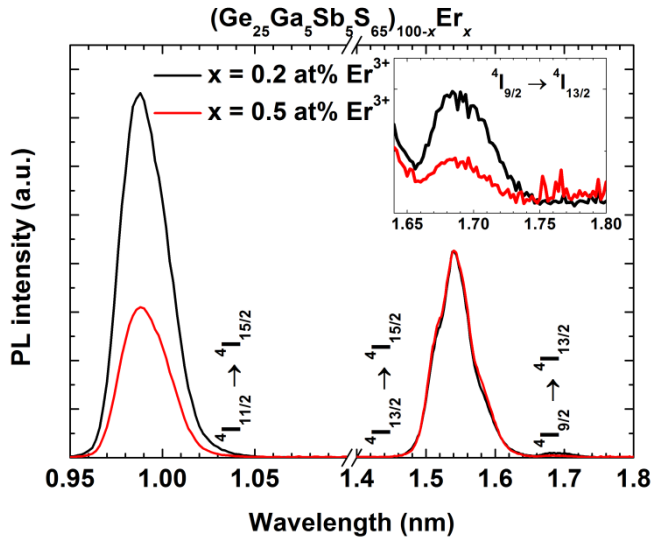


Figure 7. Stokes emission spectra in $(\text{Ge}_{25}\text{Ga}_5\text{Sb}_5\text{S}_{65})_{100-x}\text{Er}_x$, where $x = 0.2$ and 0.5 at% Er^{3+} ions pumped with 802 nm laser.

We presented visible green and red photon up-conversion emissions in $(\text{Ge}_{25}\text{Ga}_5\text{Sb}_5\text{S}_{65})_{100-x}\text{Er}_x$ amorphous chalcogenides, where $x = 0.2$ and 0.5 at% of Er^{3+} ions at pumping wavelength of 802 nm. Three observed up-conversion emission bands originate from $^2\text{H}_{11/2} \rightarrow ^4\text{I}_{15/2}$ ($\lambda \approx 530$ nm), $^4\text{S}_{3/2} \rightarrow ^4\text{I}_{15/2}$ ($\lambda \approx 550$ nm) and $^4\text{F}_{9/2} \rightarrow ^4\text{I}_{15/2}$ ($\lambda \approx 660$ nm) intra- $4f$ electronic transitions in Er^{3+} ions. The sample with 0.5 at% of Er^{3+} ions exhibits a higher intensity of red photon up-conversion emission in comparison with green photon up-conversion emission which is the reverse property than was observed for the sample doped with 0.2 at% Er^{3+} .

The dependence of pumping power density on the up-conversion emission intensities was also studied. It was found that with increase of pumping power the red photon up-conversion emission intensity increased faster than the green photon up-conversion and this red up-conversion emission intensity increased faster and more rapidly in the sample doped with higher content of Er^{3+} ions. Probably, the inter-ionic distance, reabsorption processes from a host matrix, thermal effects can play a crucial role in the observed behavior.

We believe that photon up-conversion emission intensity can be further enhanced e.g. by using the glass-ceramic samples [30], by fabrication of photonic crystals on the surface [31], by co-doping with other rare-earth ions [32].

MATERIALS AND METHODS

Chalcogenide glasses $(\text{Ge}_{25}\text{Ga}_5\text{Sb}_5\text{S}_{65})_{100-x}\text{Er}_x$, where $x = 0.2$ and 0.5 at.% were synthesized by a conventional melt-quenching technique using high purity elements of Ge (5N), Ga (5N), Sb (5N), S (4.5N) and Er (3N). Appropriate elements were loaded into silica ampoule in a glove box with dry argon atmosphere and sealed at residual pressure of $\sim 10^{-3}$ Pa. Silica tube with raw elements was put into a rocking furnace and heated at 1243 K for 24 h. The melt was water quenched and the as-prepared glass, still in the ampoule, was annealed at 20 K below the glass transition temperature (T_g) for 3 h. Then the sample was slowly cooled down to room temperature. The synthesized bulk glasses were cut into discs with a diameter ≈ 10 mm and a thickness ≈ 3 mm. Discs were shaped into rectangles and four sides were polished to optical quality.

The amorphous state of prepared samples was confirmed by X-ray diffraction (XRD) using the Bruker AXE D8-Advance diffractometer with Cu $K\alpha$ radiation source and a secondary graphite monochromator. The chemical composition

was verified by energy dispersive X-ray (EDX) microanalyzer IXRF System with a detector GRESHAM Sirius 10 and accelerating voltage of primary electron beam was 20 kV on EDX JEOL JSM-5500LV. Differential scanning calorimetry was used for determination of T_g using the TA Instruments Q2000 calorimeter. The powdered samples were measured under nitrogen, gas flow of 50 mL min^{-1} in temperature range of 623–773 K with a heating rate of 3 K min^{-1} . T_g was evaluated at the inflex point.

Absorption spectra of studied sample were measured by UV/Vis/NIR spectrophotometer JASCO V-570 in the spectral range of 400–2 000 nm with step of 2 nm. This method was used in order to determine the Er^{3+} : $^4\text{I}_{15/2} \rightarrow ^2\text{S}+^1\text{L}_J$ electronic transitions from a ground energy level of Er^{3+} : $^4\text{I}_{15/2}$. Photoluminescence spectra were measured in the spectral range of 500–2 000 nm. Samples were excited with a cw Ti:sapphire tunable laser pumped with Nd:YVO₄ laser. The pumping wavelength was 802 nm and diameter of laser beam was ~ 1 mm. Up-conversion spectra were measured at various pumping powers from 100 mW to 450 mW. The emission signal was detected under 90° with respect to the propagation of the excitation laser beam. The signal was processed through a computer-controlled 1/4 m grating monochromator with using either the photo-multiplier tube for measurement of up-conversion emission in visible spectral range or germanium detector for measurement in the near-infrared spectral region.

ACKNOWLEDGEMENT

The authors gratefully acknowledge the support from the project CZ.1.07/2.3.00/20.0254 "ReAdMat - Research Team for Advanced Non-Crystalline Materials" co-financed by the European Social Fund and the state budget of the Czech Republic, Grant Agency of the Czech Republic grant 203/09/0827, project KONTAKT II no. LH11101. The authors thank Dr. Jiri Orava (University of Cambridge) for fruitful discussion.

REFERENCES

- [1] A. Tverjanovich, Y. G. Grigoriev, S. V. Degtyarev, A. V. Kurochkin, A. A. Man'shina, Y. S. Tver'yanovich, Up-conversion fluorescence in Er-doped chalcogenide glasses based on $\text{GeS}_2\text{-Ga}_2\text{S}_3$ system, *J. Non-Cryst. Solids* **286**, 89–92 (2001).
- [2] H. T. Amorim, M. T. De Araujo, E. A. Gouveia, A. S. Gouveia-Neto, J. A. Medeiros Neto, A. S. B. Sombra, Infrared to visible up-conversion fluorescence spectroscopy in Er^{3+} -doped chalcogenide glass, *J. Lumin.* **78**, 271–277 (1998).
- [3] F. Prudenzano, L. Mescia, L. Allegretti, V. Moizan, V. Nazabal, F. Smektala, Theoretical study of cascade laser in erbium-doped chalcogenide glass fibers, *Opt. Mater.* **33**, 241–245 (2010).
- [4] F. Prudenzano, L. Mescia, L. A. Allegretti, M. De Sario, T. Palmisano, F. Smektala, V. Moizan, V. Nazabal, J. Troles, Design of Er^{3+} -doped chalcogenide glass laser for MID-IR application, *J. Non-Cryst. Solids* **355**, 1145–1148 (2009).
- [5] N. G. Boetti, J. Lousteau, D. Negro, E. Mura, G. Scarpignato, S. Abrate, D. Milanese, Multiple visible emissions by means of up-conversion process in a microstructured tellurite glass optical fiber, *Opt. Express* **20**, 5409–5418 (2012).
- [6] C. Koughia, M. G. Brik, G. Soundararajan, S. Kasap, Optical properties of $\text{Ge}_{25}\text{Ga}_{6.2}\text{Sb}_{6.3}\text{Er}_{0.5}$ glass: Stark levels and optical gain coefficient, *J. Non-Cryst. Solids* **377**, 90–94 (2013).
- [7] J. Le Person, F. Colas, C. Compère, M. Lehaitre, M. L. Anne, C. Boussard-Plédel, B. Bureau, J. L. Adam, S. Deputier, M. Guilloux-Viry, Surface plasmon resonance in chalcogenide glass-based optical system, *Sensor. Actuat. B-Chem.* **130**, 771–776 (2008).
- [8] F. Charpentier, B. Bureau, J. Troles, C. Boussard-Plédel, K. Michel-Le Pierres, F. Smektala, J. L. Adam, Infrared monitoring of underground CO₂ storage using chalcogenide glass fibers, *Opt. Mater.* **31**, 496–500 (2009).
- [9] A. V. Rode, A. Zakery, M. Samoc, R. B. Charters, E. G. Gamaly, B. Luther-Davies, Nonlinear as-s chalcogenide films for optical waveguide writing deposited by high-repetition-rate laser ablation, *Appl. Surf. Sci.* **197–198**, 481–485 (2002).
- [10] F. Prudenzano, L. Mescia, L. Allegretti, M. De Sario, F. Smektala, V. Moizan, V. Nazabal, J. Troles, J. L. Doualan, G. Canat, J. L. Adam, B. Boulard, Simulation of mid-IR amplification in Er^{3+} -doped chalcogenide microstructured optical fiber, *Opt. Mater.* **31**, 1292–1295 (2009).
- [11] B. Bureau, X. H. Zhang, F. Smektala, J. L. Adam, J. Troles, H.-I. Ma, C. Boussard-Plédel, J. Lucas, P. Lucas, D. Le Coq, M. R. Riley, J. H. Simmons, Recent advances in chalcogenide glasses, *J. Non-Cryst. Solids* **345–346**, 276–283 (2004).
- [12] A. B. Seddon, Chalcogenide glasses: a review of their preparation, properties and applications, *J. Non-Cryst. Solids* **184**, 44–50 (1995).
- [13] A. Zakery, S. R. Elliott, Optical properties and applications of chalcogenide glasses: a review, *J. Non-Cryst. Solids* **330**, 1–12 (2003).
- [14] K. Tanaka, K. Shimakawa, *Amorphous chalcogenide semiconductors and related materials*, Springer, 2011.
- [15] R. Fairman, B. Ushkov, *Semiconducting chalcogenide glass III: Applications of chalcogenide glasses*, Elsevier Science, 2004.
- [16] B. Walsh, Judd-Ofelt theory: Principles and practices, in *Advances in spectroscopy for lasers and sensing*, (Eds. B. Di Bartolo, O. Forte), Springer Netherlands, 2006, pp. 403–433.

- [17] A. Tverjanovich, Y. G. Grigoriev, S. V. Degtyarev, A. V. Kurochkin, A. A. Man'shina, T. Y. Ivanova, A. Povolotskiy, Y. S. Tveryanovich, Up-conversion luminescence efficiency in Er-doped chalcogenide glasses, *J. Non-Cryst. Solids* **326–327**, 311–315 (2003).
- [18] K. Kadono, T. Yazawa, S. Jiang, J. Porque, B.-C. Hwang, N. Peyghambarian, Rate equation analysis and energy transfer of Er³⁺-doped Ga₂S₃-GeS₂-La₂S₃ glasses, *J. Non-Cryst. Solids* **331**, 79–90 (2003).
- [19] K. Kadono, H. Higuchi, M. Takahashi, Y. Kawamoto, H. Tanaka, Upconversion luminescence of Ga₂S₃-based sulfide glasses containing Er³⁺ ions, *J. Non-Cryst. Solids* **184**, 309–313 (1995).
- [20] L. Strizik, J. Zhang, T. Wagner, J. Oswald, T. Kohoutek, B. M. Walsh, J. Prikryl, R. Svoboda, C. Liu, B. Frumarova, M. Frumar, M. Pavlista, W. J. Park, J. Heo, Green, red and near-infrared photon up-conversion in Ga-Ge-Sb-S:Er³⁺ amorphous chalcogenides, *J. Lumin.* **147**, 209–215 (2014).
- [21] Y. Guimond, J.-L. Adam, A.-M. Jurdyc, H. L. Ma, J. Mugnier, B. Jacquier, Optical properties of antimony-stabilised sulphide glasses doped with Dy³⁺ and Er³⁺ ions, *J. Non-Cryst. Solids* **256–257**, 378–382 (1999).
- [22] J. Ren, T. Wagner, J. Oswald, J. Orava, B. Frumarova, M. Frumar, Spectroscopic properties of Ni²⁺ and rare-earth codoped Ge-Ga-Sb-S glass, *J. Phys. Chem. Solids* **71**, 30–34 (2010).
- [23] T. H. Lee, S. I. Simdyankin, J. Hegedus, J. Heo, S. R. Elliott, Spatial distribution of rare-earth ions and GaS₄ tetrahedra in chalcogenide glasses studied via laser spectroscopy and ab initio molecular dynamics simulation, *Phys. Rev. B* **81**, 104204 (2010).
- [24] J. Heo, J. M. Yoon, S. Y. Ryou, Raman spectroscopic analysis on the solubility mechanism of La³⁺ in GeS₂-Ga₂S₃ glasses, *J. Non-Cryst. Solids* **238**, 115–123 (1998).
- [25] D. Gamelin, H. Güdel, Upconversion processes in transition metal and rare earth metal systems, in *Transition metal and rare earth compounds* (Ed. H. Yersin), Springer Berlin Heidelberg, 2001, pp. 1–56.
- [26] M. Pollnau, D. R. Gamelin, S. R. Lüthi, H. U. Güdel, M. P. Hehlen, Power dependence of upconversion luminescence in lanthanide and transition-metal-ion systems, *Phys. Rev. B* **61**, 3337–3346 (2000).
- [27] S. R. Lüthi, M. Pollnau, H. U. Güdel, M. P. Hehlen, Near-infrared to visible upconversion in Er³⁺-doped Cs₃Lu₂Cl₉, Cs₃Lu₂Br₉, and Cs₃Y₂I₉ excited at 1.54 μm, *Phys. Rev. B* **60**, 162–178 (1999).
- [28] L. Li, Z.-X. Zhou, W.-L. Yang, H. Li, Y. Wu, Upconversion emission properties of erbium- and ytterbium-doped potassium lithium tantalate niobate ceramics, *Chinese Phys. Lett.* **30**, 127103 (2013).
- [29] A. Bednarkiewicz, D. Wawrzynczyk, M. Nyk, M. Samoć, Tuning red-green-white up-conversion color in nano NaYF₄:Er/Yb phosphor, *J. Rare Earth* **29**, 1152–1156 (2011).
- [30] R. Balda, S. García-Revilla, J. Fernández, V. Seznec, V. Nazabal, X. H. Zhang, J. L. Adam, M. Allix, G. Matzen, Upconversion luminescence of transparent Er³⁺-doped chalcogenide glass-ceramics, *Opt. Mater.* **31**, 760–764 (2009).
- [31] M. E. Pollard, K. J. Knight, G. J. Parker, D. W. Hewak, M. D. B. Charlton, Fabrication of photonic crystals in rare-earth doped chalcogenide glass films for enhanced upconversion, *Proc. SPIE* **8257**, 82570V (2012).
- [32] S. F. Felix, E. A. Gouveia, M. T. de Araujo, A. S. B. Sombra, A. S. Gouveia-Neto, Up-conversion pumped light amplification with temperature tunable gain in Er³⁺/Yb³⁺-codoped chalcogenide glasses, *J. Lumin.* **87–89**, 1020–1022 (2000).